

The Nansen Environmental and Remote Sensing Center

a non-profit
research institute affiliated with
the University of Bergen



Edv. Griegsvei 3a,
N-5059 Solheimsviken
Norway

NERSC Technical Report no.210

Annual Report of RADARC

by

Yongqi Gao, Helge Drange, Mats Bentson,
Ola M. Johannessen, Lasse Petersson

Bergen, January 19, 2002

Title: Annual Report of RADARC, 2001	Report No. 210
Client: NERSC	Contract No. ICA2-CT-2000-10037
Contact Person: Ola M. Johannessen	Availability:
Authors: Gao et al.	Date: January 19, 2002
Approval:	Ola M. Johannessen, Director

Nansen Environmental and Remote Sensing Center

Edvard Griegsvei 3a

N-5059 Bergen

Norway

Phone: +47 55297288 Fax: +47 55200050

E-mail: administrasjon@nersc.no Web: <http://www.nersc.no>

Draft for Deliverable D.6

1 Introduction of WP5

An existing 3-D coupled ocean and sea ice model will be used to include the transport and dispersal of radionuclides. The coupled ocean-sea ice-radionuclides model will then be validated against the observed pathway and distributions of the radionuclides.

The specific tasks in WP5 are as follows (also see the Proposal):

Subtask 1. Modifications, testing and validation of an existing tracer advection and dispersal module online coupled to the North Atlantic-Arctic model;

Subtask 2. Coding and testing of a module describing the input of various terrestrial and atmospheric sources of radionuclides;

Subtask 3. Identification and interpolation of data sets for validation of simulated radionuclides transport and dispersal; and

Subtask 4. Validation of the simulated radionuclides transport and dispersal fields.

2 Model Description

2.1 MICOM

MICOM (Bleck et al., 1992), with potential density as the vertical coordinate, is a primitive equation ocean model and it is used as the ocean circulation model in the RADARC project. The modelled ocean consists of a surface mixed layer (ML) in which the potential density varies in time and space, and several interior isopycnal layers. The top mixed layer utilizes the Gaspar (1988) parameterization for the dissipation of turbulent kinetic energy. All the air-sea exchanges of momentum, heat and fresh water are incorporated into the mixed layer. Convective mixing takes place if the density of the surface ML exceeds the density of one or more of the underlying isopycnals. The instability is removed by mixing all of the unstable water masses with the ML water, and by absorbing the new water mass into the ML. Both momentum and tracers (temperature, salinity and the radionuclides) are uniformly mixed in the case of convective mixing. The interior layers exchange their properties with the ML if they outcrop into the ML. The equations are discretised on an Arakawa and Lamb (1977) C-grid stencil. The basic version of MICOM is documented in Bleck et al. (1992).

Configuration of MICOM

A global version of MICOM has been configured at NERSC and is used in the RADARC project. In the horizontal, a local orthogonal grid system with two poles over northern hemisphere has been adopted (Bentsen et al., 1999). The variation of the horizontal grid resolution (Fig. 1) favors the requested simulation on the Nordic Seas and the Arctic Ocean in the project, where the grid scale is about 50 km. There are 26 layers in the

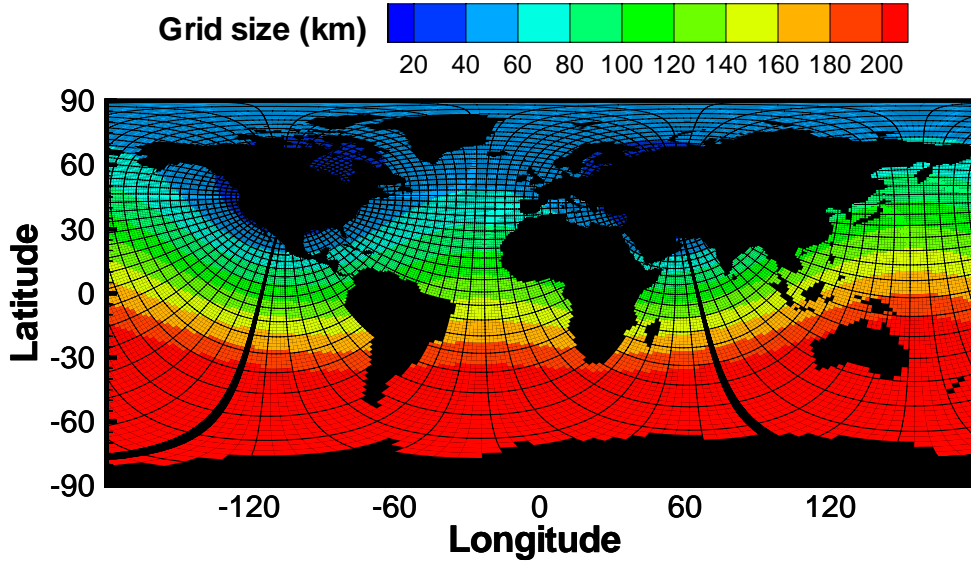


Figure 1: The horizontal grid layout (each line represents 5 grid cells in the model) and grid size (color; km) applied in the experiments.

vertical and the specified potential densities of the sub-surface layers were chosen to ensure proper representation of the major water masses in the North Atlantic/Nordic Sea region. The densities of the isopycnic layers (in σ_0 -units) are 24.12, 24.70, 25.28, 25.77, 26.18, 26.52, 26.80, 27.03, 27.22, 27.38, 27.52, 27.63, 27.71, 27.77, 27.82, 27.86, 27.90, 27.94, 27.98, 28.01, 28.04, 28.07, 28.10, 28.85 and 29.10.

The vertically homogeneous ML utilises the Gaspar (1988) bulk parameterisation for the dissipation of turbulent kinetic energy, and has temperature, salinity and layer thickness as the prognostic variables. In the isopycnic layers below the ML, temperature and layer thickness are the prognostic variables, whereas the salinity is diagnostically determined by means of the simplified equation of state of Friedrich and Levitus (1972). The bathymetry is computed as the arithmetic mean value based on the ETOPO-5 data base (from National Geophysical Data Center, USA).

The thermodynamic sea ice module incorporates freezing and melting of sea ice and snow covered sea ice (Drange & Simonsen, 1996), and is based on the thermodynamics of Semtner Jr. (1976), Parkinson and Washington (1979) and Fichefet and Gaspar (1988). The dynamic part of the sea ice module is based on the viscous-plastic rheology of Hibler (1979), where sea ice is considered as a two-dimensional continuum. The dynamic ice module has been further modified by Harder (1996) to include description of sea ice roughness and the age of sea ice, and utilising the advection scheme of Smolarkiewicz (1984).

Set-up and Spin-up of MICOM

The diffusive velocities (diffusivities divided by the size of the grid cell) for layer interface diffusion, momentum dissipation, and tracer dispersion are 0.01 m s^{-1} , 0.02 m s^{-1} and 0.01 m s^{-1} , respectively, yielding actual diffusivities of about $10^3 \text{ m}^2 \text{ s}^{-1}$. The model simulation was initialised by the January Levitus and Boyer (1994) and Levitus et al. (1994) climatological temperature and salinity fields, respectively, a 2 m thick sea ice cover based on the climatological sea ice extent (Lisaeter et al., 2001), and an ocean at rest. The model was then integrated for 180 years by applying the monthly mean NCAR/NCEP atmospheric forcing fields, surface temperature and salinity relaxation. The quasi-global and global versions of MICOM with tracer module included have already been used to investigate the uptake and ventilation of the chlorofluorocarbons (CFC-11 and CFC-12) in the recently-ended EC Project Global Oceanic Storage of the Anthropogenic Carbon (GOSAC) (Dutay et al., 2001; Gao et al., 2001). The obtained results indicate that the model is able to produce fairly realistic tracer fields in the North Atlantic and the Nordic Seas regions.

2.2 The Tracer Model

The equation for the transport and mixing of the radionuclides is shown below, which without radioactive decay is the same as that for temperature and salinity in MICOM.

$$\frac{\partial}{\partial t} \left(\frac{\partial p}{\partial s} C \right) + \underbrace{\nabla_s \cdot (\vec{v} \frac{\partial p}{\partial s} C)}_{\text{advection}} + \underbrace{\frac{\partial}{\partial s} \left(\dot{s} \frac{\partial p}{\partial s} C \right)}_{\text{mass transfer}} = \underbrace{\nabla_s \cdot \left(\nu_1 \frac{\partial p}{\partial s} \nabla_s C \right)}_{\text{diffusion}} + \underbrace{\kappa_C}_{\text{source/sink}} - \underbrace{\lambda}_{\text{decay}} \quad (1)$$

Here p is the pressure, C is the concentrations of the tracers, \vec{v} is the isopycnal velocity, s is the vertical coordinate, and ν_1 is the diffusive velocity for the tracers. The decay term is implemented using the radioactive decay constant for the radionuclides.

3 Radionuclides Simulations for Validation Purpose

3.1 Implementation of Radionuclides Simulations

Source of Radionuclides

In terms of contribution to the marine environment, the atmospheric fallout and the European reprocessing plants are the most important sources (Nies et al., 1998). Therefore, two major sources of the radionuclides are implemented. One is the atmospheric fallout from the nuclear bomb testing, which provide the present “background” concentration in the surface waters of the Nordic Seas, and the other is the Sellafield release, which has been one of the most important sources of radioactive contamination in the Arctic Ocean since 1970s (Strand et al., 1996). The Sellafield signal has been intensively observed in the last decade and these source and distribution data have been utilized for the model validation.

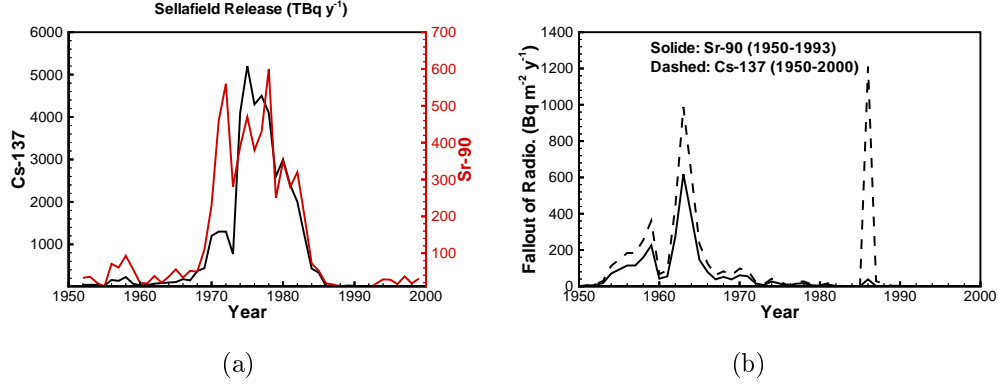


Figure 2: The time evolution of ^{137}Cs and ^{90}Sr in (a) the Sellafield release (unit: TBq y^{-1}) and (b) the atmospheric fallout (unit: $\text{Bq m}^{-2} \text{y}^{-1}$) in Denmark.

Radionuclides

In the RADARC project, the transport and mixing of Caesium-137 (^{137}Cs) and Strontium-90 (^{90}Sr) will be simulated. Both radionuclides are soluble in sea water and can be considered as passive tracers with a similar half-life of 30.1 and 29 years, respectively. The time evolution of ^{137}Cs and ^{90}Sr of the Sellafield release and for the atmospheric fallout in Denmark (Nilsen [pers. comm.]) is prescribed and shown in Fig. 2. The latitudinal distribution of the atmospheric ^{90}Sr deposition (UNSCEAR, 1982, Fig. 3) makes it feasible to construct the source function of the atmospheric fallout globally. A total of four tracers are designed, they are atmospheric fallout of ^{137}Cs and ^{90}Sr , and the Sellafield discharge of ^{137}Cs and ^{90}Sr .

3.2 RADARC Simulations

In the hindcast simulation, the ocean model is forced with daily atmospheric fields provided by the NCAR/NCEP reanalysis project (Kalnay et al., 1996). In this integration, the ML salinity is relaxed towards a diagnosed salt flux. The physical model was initialised from a 180 yr spin-up integration using monthly climatological forcing fields. The initial fields of the radionuclides from the atmospheric fallout and the Sellafield discharge are zero. The simulation begins in 1950 and ends in 1999. For the forthcoming predictions, namely the Control and the 2^*CO_2 Runs, the model will be forced by the atmospheric forcing fields from a coupled air-sea-ice climate model (from the Bergen Climate Model or from Max-Planck Climate Model, for instance, covering the period 2000-2100).

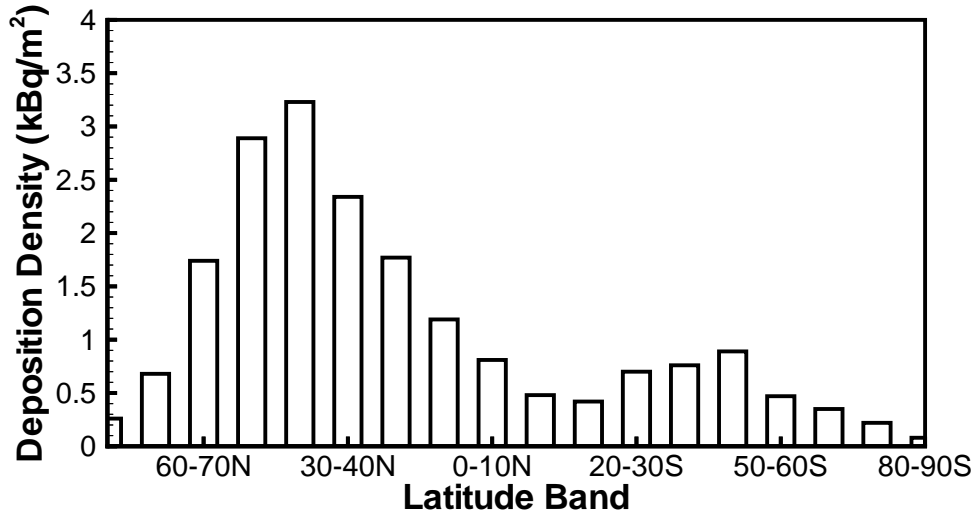


Figure 3: Atmospheric deposition of ⁹⁰Sr (kBq m⁻²) vs. latitude (UNSCEAR, 1982).

3.3 Test Simulation

A test simulation, in which the model horizontal grid resolution is half of the resolution of the hindcast run (about 100 km in the Nordic Seas), has been completed, and some of the obtained results are presented here.

3.4 Results from the Test simulation

Pathway of the Sellafield Discharge

Before flowing northward with the Norwegian Coastal Current (NCC), the simulated Sellafield radionuclides circulate cyclonically in the North Sea (see Fig. 4). One branch enters the Barents Sea, and one branch heads for the Fram Strait following the West Spitzbergen Current (WSC). The simulated pathway of the Sellafield release to the Barents Sea is consistent with observations (Kershaw & Baxter, 1995). In the Barents Sea, the Sellafield signal spreads to north-east and reaches the Arctic Ocean. The simulated Sellafield signal passes the Denmark Strait via the East Greenland Current (EGC) in year 1975 and reaches the Labrador Sea in year 1980. It should be noted that the Sellafield signal does not go eastward from the Barents Sea, instead, the signal goes to westward following the Canadian Archipelago in year 1985. The dispersal of the Sellafield signal is, of course, closely associated with the simulated circulation field in the region (Fig. 5).

To qualitatively and quantitatively check the simulated dispersal of the Sellafield discharge, we show the time series of the simulated surface ¹³⁷Cs concentration East of Scotland (57.0-57.5°N, 1.5-2.0°W), West of Norway (59-61°N, 3.5-5.0°E) and in the

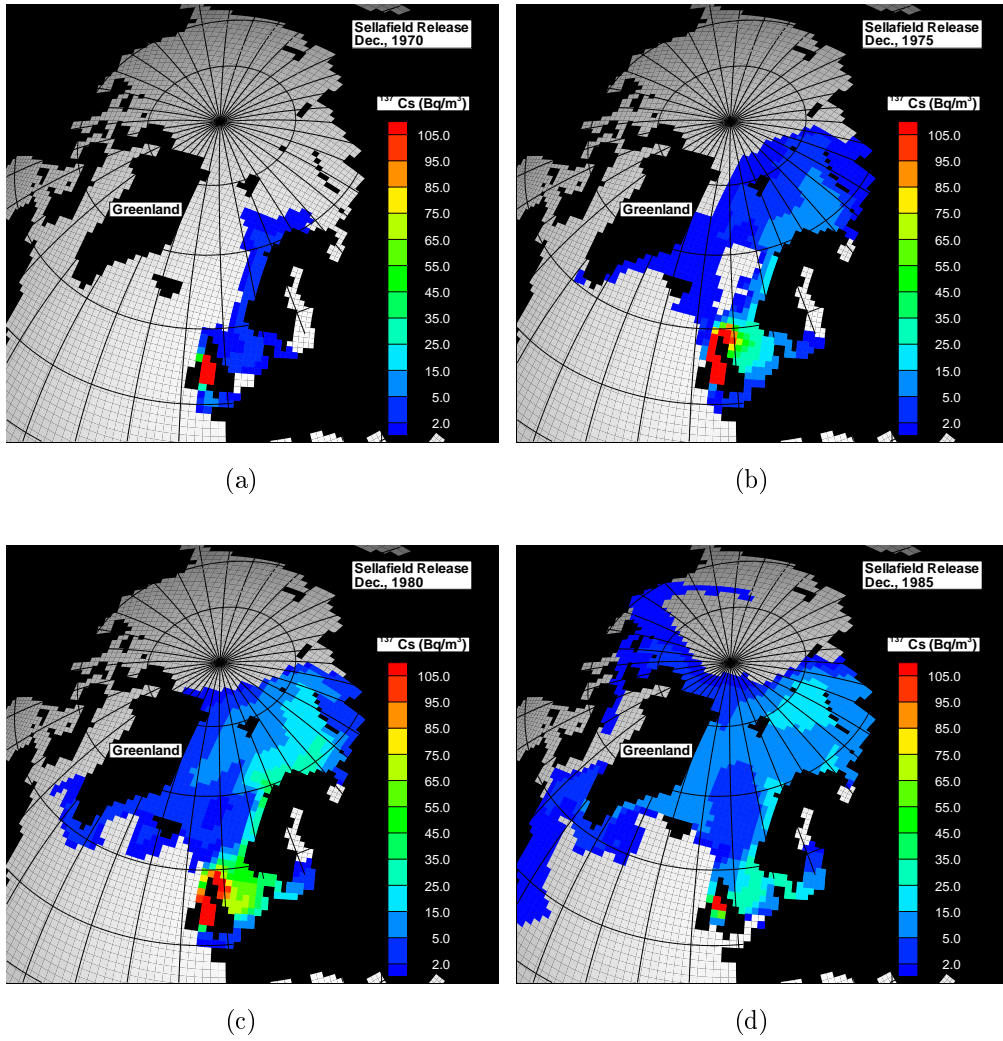
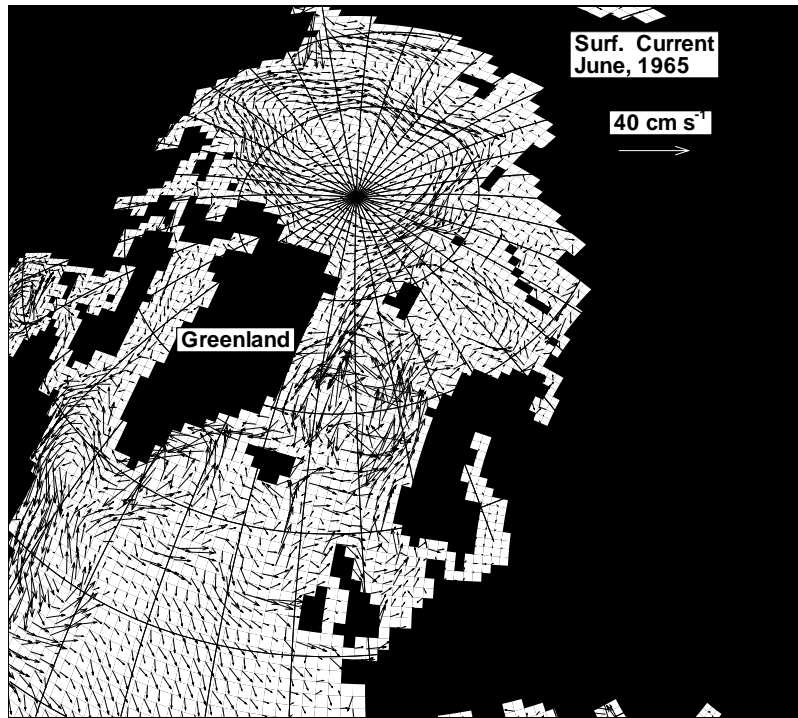
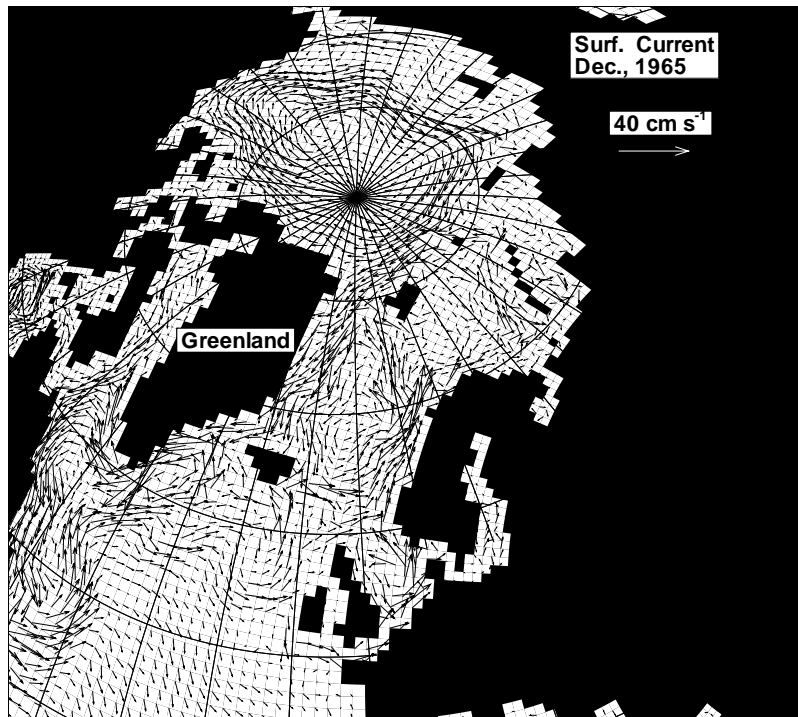


Figure 4: Simulated surface concentration of ^{137}Cs (Bq m $^{-3}$) in (a) December 1970, (b) December 1975, (c) December 1980, and (d) December 1985 due to the Sellafield release. The cut off value is 1 Bq m $^{-3}$.



(a)



(b)

Figure 5: Simulated surface currents in (a) June 1965 and (b) December 1965.

South-West Barents Sea region (71-72°N, 20-30°E) in Fig. 6, superimposed on a histogram of the annual mean discharges. Clearly, the global fallout dominates the surface ^{137}Cs distribution in mid-1960s in the three regions. From late 1970s to late 1980s, the Sellafield discharges dominates the surface ^{137}Cs distribution.

The simulated variation of the surface ^{137}Cs concentrations are in broad agreement with the observations (Kershaw & Baxter, 1995; data is not shown here for the regions East of Scotland and West of Norway). It follows that the simulated surface ^{137}Cs concentrations are lower than the observed values, for instance, the maximum concentration in the Barents Sea is about 75% of the observed value.

The simulated transit times for the Sellafield release are 2 years to East of Scotland, 4 years to West of Norway and 4-5 years to the South-West Barents Sea. Here the transit time is defined as the difference in time when the maximum concentration occurs in the specific region and when the maximum Sellafield release happened. These simulated transit times are in good agreement with the earlier studies (Kershaw & Baxter, 1995; Livingston et al., 1984).

4 Outlook

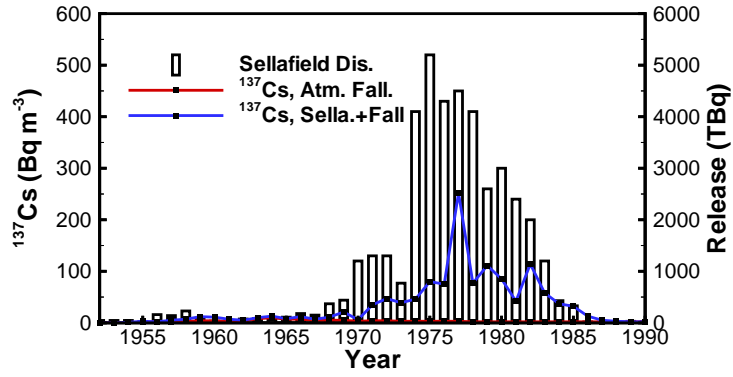
The hindcast simulation will begin as soon as the selected “release” scenarios are available. The Control and 2*CO₂ Runs will begin after the hindcast simulation is finished.

5 Requirement for Future Simulations

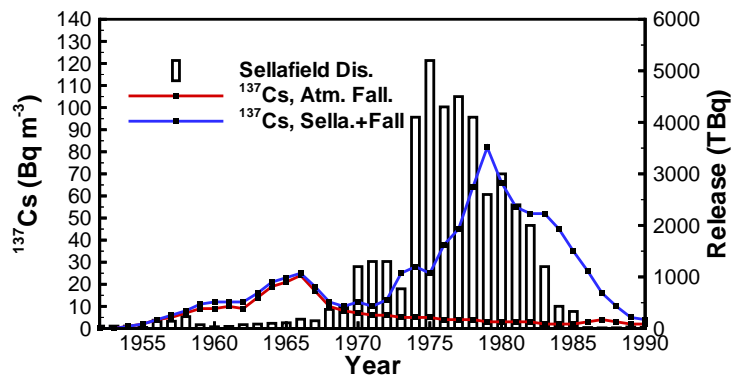
The selected “release” scenarios are necessary for the future simulations. To be specific, the location of the release point (lat/lon/depth) and the time evolution of the release flux are needed. If possible, the data in ascii format is appreciated.

References

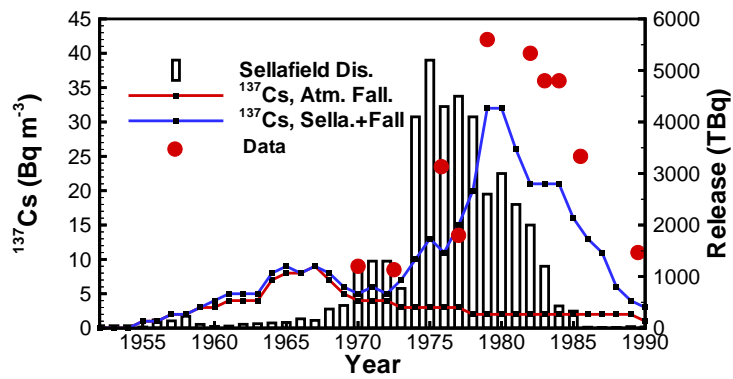
- Arakawa, A., & Lamb, V. (1977). Computational design of the basic processes of the UCLA General Circulation Model. *Methods Comput. Phys.*, *17*, 174-265.
- Bentsen, M., Evensen, G., Drange, H., & Jenkins, A. D. (1999). Coordinate Transformation on a Sphere Using Conformal Mapping. *Mon. Wea. Rev.*, *127*, 2733-2740.
- Bleck, R., Rooth, C., Hu, D., & Smith, L. T. (1992). Salinity-driven Thermocline Transients in a Wind- and Thermohaline-forced Isopycnic Coordinate Model of the North Atlantic. *J. Phys. Oceanogr.*, *22*, 1486-1505.
- Drange, H., & Simonsen, K. (1996). *Formulation of air-sea fluxes in the ESOP2 version of MICOM* (Tech. Rep. No. 125). Edv. Griegsv. 3A, N-5037 Solheimsviken, Norway: Nansen Environmental and Remote Sensing Center.
- Dutay, J., Bullister, J., Doney, S., Orr, J., Najjar, R., Caldeira, K., Campin, J., Drange, H., Follows, M., Gao, Y., Gruber, N., Hecht, M., Ishida, A., Joos, F., Lindsay, K., Madec, G., Marier-Reimer, E.,



(a)



(b)



(c)

Figure 6: Time series of the simulated surface concentration of ^{137}Cs (Bq m^{-3}) for (a) East of Scotland, (b) West of Norway and (c) in the South-West Barents Sea region. Observed data in (c) is from Kershaw and Baxter (1995). Note the different concentration scales on the panels.

- Marshall, J., Matear, R., Monfray, P., Plattner, G., Sarmiento, J., Schlitzer, R., Slater, R., Totterdell, I., Weirig, M., Yamanaka, Y., & Yool, A. (2001). Evaluation of ocean model ventilation with CFC-11: comparison of 13 global ocean models. *Ocean Modelling*. (in press)
- Fichefet, T., & Gaspar, P. (1988). A model study of upper ocean-sea ice interaction. *J. Phys. Oceanogr.*, *18*, 181–195.
- Friedrich, H., & Levitus, S. (1972). An approximation to the equation of state for sea water, suitable for numerical ocean models. *J. Phys. Oceanogr.*, *2*, 514–517.
- Gao, Y., Drange, H., & Bension, M. (2001). The Ventilation of the Intermediate and Deep Atlantic Ocean Deduced from the Spatial and Temporal Distribution of CFCs in a Global Isopycnic Coordinate Ocean Model. (Re-submitted to Ocean Modelling)
- Gaspar, P. (1988). Modeling the seasonal cycle of the upper ocean. *J. Phys. Oceanogr.*, *18*, 161–180.
- Harder, M. (1996). *Dynamik, Rauhgigkeit und Alter des Meereises in der Arktis*. Unpublished doctoral dissertation, Alfred-Wegener-Institut für Polar- und Meeresforschung, Bremerhaven, Germany.
- Hibler, W. (1979). A dynamic thermodynamic sea ice model. *J. Phys. Oceanogr.*, *9*, 815–846.
- Kalnay, E., Kanamitsu, M., Kistler, R., Collins, W., Deaven, D., Gandin, L., Iredell, M., Saha, S., White, G., Woollen, J., Zhu, Y., Chelliah, M., Ebisuzaki, W., Higgins, W., Janowiak, J., Mo, K. C., Ropelewski, C., Leetmaa, A., Reynolds, R., & Jenne, R. (1996). The NCEP/NCAR Reanalysis Project. *Bull. Amer. Meteor. Soc.*, *77*, 437–471.
- Kershaw, P., & Baxter, A. (1995). The transfer of reprocessing wastes from north-west Europe to the Arctic. *Deep Sea Res.*, *42*, 1413–1448.
- Levitus, S., & Boyer, T. P. (1994). *World Ocean Atlas 1994 Volume 4: Temperature*. Washington, D.C.: NOAA Atlas NESDIS 4.
- Levitus, S., Burgett, R., & Boyer, T. P. (1994). *World Ocean Atlas 1994 Volume 3: Salinity*. Washington, D.C.: NOAA Atlas NESDIS 3.
- Lisaeter, K., Johannessen, O., Drange, H., Evensen, G., & Sandven, S. (2001). Comparison of modeled and observed sea ice concentration and thickness fields in the Arctic. *J. Geophys. Res.* (Submitted)
- Livingston, H., Kupferman, S., Bowen, V., & Moore, R. (1984). Vertical profile of artificial radionuclide concentrations in the central Arctic Ocean. *J. Geophys. Res.*, *89*, 2195–2203.
- Nies, H., Harms, H., Karcher, M., Dethleff, D., Bahe, C., Kuhlmann, G., Oberhuber, J., Backhaus, J., Kleine, E., Loewe, P., Matishov, D., Stepanov, A., & Vasiliev, O. (1998). Anthropogenic Radioactivity in the Nordic Seas and the Arctic Ocean - Results of a Joint Project. *Deutsche Hydrographische Zeitschrift*, *50*(4), 313–343.
- Parkinson, C. L., & Washington, W. M. (1979). A Large-Scale Numerical Model of Sea Ice. *J. Geophys. Res.*, *84*, 311–337.
- Semntner Jr., A. J. (1976). A model for the thermodynamic growth of sea ice in numerical investigations of climate. *J. Phys. Oceanogr.*, *6*, 379–389.
- Smolarkiewicz, P. K. (1984). A Fully Multidimensional Positive Definite Advection Transport Algorithm with Small Implicit Diffusion. *J. Comp. Phys.*, *54*, 325–362.
- Strand, P., Aarkrog, A., Bowers, J., Tsaturov, Z., & Magnusson, S. (1996). Radioactive Contamination of the Arctic Marine Environment. In *Radionuclides in the Oceans - Inputs and Inventories* (p. 95–119). Inst. de Protection et de Surete Nucleaire, France.
- UNSCEAR. (1982). Ionizing Radiation: Sources and Biological Effects. In *Unscear 1982 report to the general assembly with scientific annexes*. United Nations, New York: United Nations Scientific Committee on the Effects of Atomic Radiation.